Available online at www.sciencedirect.com

SCIENCE DIRECT®

ELSEVIER

Tribology International ▮ (▮▮▮▮) ▮▮▮–▮▮▮

TRIBOLOGY INTERNATIONAL

www.elsevier.com/locate/triboint

The effect of lateral vibrations on transport and friction in nanoscale contacts

Z. Tshiprut[a,*], A.E. Filippov[b], M. Urbakh[a]

[a]School of Chemistry, Tel Aviv University, 69978 Tel Aviv, Israel
[b]Donetsk Institute for Physics and Engineering of NASU, 83144, Donetsk, Ukraine

Abstract

We demonstrate that lateral vibrations of a substrate can dramatically increase surface diffusivity and mobility and reduce friction at the nanoscale. In contrast to the enhancement of diffusion and mobility that has a resonance nature, the reduction of friction does not exhibit pronounce resonance features. We find an abrupt dilatancy transition from the state with a small tip–surface separation to the state with a large separation as the vibration frequency increases. Dilatancy is shown to play an essential role in dynamics of a nanometer-size tip which interacts with a vibrating surface. Atomic force microscopy (AFM) experiments are suggested which can test the predicted effects.

Keywords: ■; ■; ■

1. Introduction

Due to its practical importance and the relevance to basic scientific questions there has been major increase in activity in studies of dynamics in nanoscale confinement during the last decade [1–4]. A substantial progress in understanding the leading factors that determine the dynamics in confining systems has opened new possibilities to modify and control motion at the nanoscale [5–15]. The difficulties in realizing an efficient control of motion are related to the complexity of the task, namely dealing with systems with many degrees of freedom under a strict size confinement, which leaves very limited access to interfere with the system in order to be able to control.

Controlling frictional forces has been traditionally approached by chemical means, namely, using lubricating liquids [16,17]. A different approach, which has attracted considerable interest recently, is by controlling the system mechanically via normal vibration of small amplitude and energy [8–11,13]. In this case, the idea is to reduce the friction force or to eliminate stick–slip motion through a stabilization of desirable modes of motion. Calculations demonstrated that oscillations of the normal load could lead to a transition from a state of high-friction stick–slip dynamics to a low-friction smooth sliding state [8,9,11,13]. These theoretical predictions have been supported by experimental studies which indicate that normal vibrations generally stabilize the system against stick–slip oscillations and lead to a substantial decrease of frictional forces [10,13]. Recently, a significant reduction of friction have also been observed by applying lateral oscillations to the cantilever holder while sliding on mica [14].

In this paper we investigate the effect of lateral vibrations of a substrate on diffusivity, mobility and friction at the nanoscale. We demonstrate that manipulations by mechanical excitations when applied at the right frequency and amplitude can dramatically increase surface diffusion and mobility and reduce friction. A preliminary account of this work has been published in Ref. [18].

The proposed approach differs from earlier suggestions of controlling friction via normal vibrations [8–11,13]. The predicted effects should be amenable to atomic force microscopy (AFM) tests using, for instance, shear modulation mode [14,19] or applying ultrasound to the sample [20,21]. The model can be also used in studies of contact mechanics of a probe interacting with oscillating quartz

*Corresponding author.

0301-679X/$ - see front matter © 2006 Published by Elsevier Ltd.
doi:10.1016/j.triboint.2006.02.055

crystal microbalance surfaces which could provide a unique information on interfacial properties under high-frequency shear [22–24].

2. The model

In order to study the effect of lateral vibrations on diffusion and friction in the context of AFM, we introduce a model of a tip interacting with a substrate, which oscillates in the lateral direction (see Fig. 1). The motion of the tip in the lateral and normal directions is governed by the coupled Langevin equations:

$$M\ddot{x}(t) = -\eta_x(z)(\dot{x}(t) - \dot{x}_0(t)) - \partial U(x - x_0, z)/\partial x + F_x + f_x \tag{1}$$

and

$$M\ddot{z}(t) = -\eta_z(z)\dot{z}(t) - \partial U(x - x_0, z)/\partial z + F_z + f_z, \tag{2}$$

where

$$U(x,z) = U_0\left[1 + \sigma \sin\left(\frac{2\pi}{b}(x - x_0)\right)\right]\exp(1 - z/\lambda) \tag{3}$$

and

$$\eta_{x,z}(z) = \eta^0_{x,z}\exp(1 - z/\lambda). \tag{4}$$

Here M and x, z are the mass and the lateral and normal coordinates of the tip, $U(x,z)$ is the potential experienced by the tip due to the interaction with the substrate, b is its periodicity in the lateral direction, and σ characterizes the amplitude of corrugation in the x-direction. The parameters η_x and η_z are responsible for the dissipation of the tip kinetic energy due to the motion in the x and z directions, respectively. These terms account for dissipation due to phonons and/or other excitations [3,15]. Here, we take into account the dependence of U and $\eta_{x,z}$ on the tip–substrate separation [11] and assume an exponential decrease of U and $\eta_{x,z}$ with a rate λ^{-1} as z increases. It should be noted that the particular form of z-dependence of the potential and dissipation parameters chosen here serves only as an example to demonstrate the suggested mechanism for tuning friction. However, our conclusions are mostly independent of the particular form of the potentials.

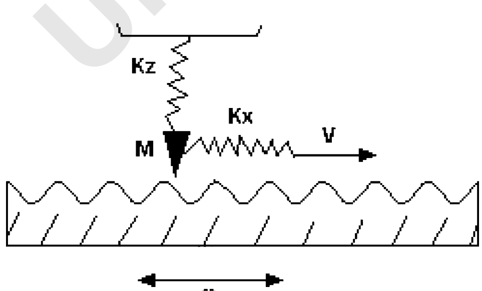

Fig. 1. Schematic sketch of the system.

The tip is held at the surface by a normal load $F_z = K_z(z_0 - z(t))$ applied by a linear spring of spring constant K_z. In friction experiments the tip is laterally pulled, $F_x = K_x(vt - x(t))$, by a spring of spring constant K_x connected to a stage which moves with a constant velocity v. The effect of lateral vibrations of the substrate is included through a time dependence of its position, $x_0 = A_0\sin(2\pi\omega t)$, where A_0 and ω are the amplitude and the frequency of the oscillations. The random forces, $f_{x,z}$, represent thermal noise satisfying the fluctuation–dissipation relation,

$$\langle f_i(t)f_j(0)\rangle = 2\eta_i k_b T\delta(t)\delta_{i,j}, \quad i,j = x,z. \tag{5}$$

It is convenient to introduce the dimensionless coordinates and time $X = x/b$, $Z = z/b$, $\tau = t\omega_0$, where $\omega_0 = (1/b)\sqrt{U_0\sigma/M}$ is the frequency of the small oscillations of the tip in the periodic potential. The dynamical behavior of the system is determined by the following dimensionless parameters: $A = A_0/b$, $\Omega = \omega/\omega_0$, $k_B T/U_0$, $\eta_{x,z}/M\omega_0$, λ/b, $K_x b^2/(4\pi^2 U_0\sigma)$, $K_z\lambda^2/U_0$ and $\tilde{v} = v/(\omega_0 b)$.

3. Results and discussion

3.1. Vibration-induced enhancement of surface diffusion

First we consider the effect of the substrate vibrations on surface diffusion, which occurs in the absence of the lateral driving force, $F_x = 0$. We start from the case of one-dimensional motion of the tip, which takes place for a stiff normal spring, $K_z \gg U_0(1+\sigma)/\lambda^2$. Then the distance between the tip and the surface is constant, $z = z_0$. Eq. (1) shows that the substrate vibrations cause a time-periodic (ac) force acting on the tip, $F_{ac} = M(2\pi\omega)^2 A_0\sin(2\pi\omega t)$. This force presents the effect of inertia. Its amplitude depends on both the amplitude and frequency of vibrations. Recent studies of surface diffusion under ac forcing [6,7] demonstrated that the diffusivity D may be strongly enhanced and even exceed the free (Brownian) diffusivity, $D_{free} = k_B T/\eta_x$, for an optimal matching of the driving frequency, ω, and the amplitude A_0. We would like to remind that in the absence of vibrations the diffusion coefficient of the tip which interacts with a surface, is exponentially smaller than D_{free}.

Our calculations also demonstrated that lateral vibrations of the substrate can drastically enhance the diffusivity of the tip. As an example we show in Fig. 2 the frequency dependence of the diffusion coefficient, $D(\Omega)$, calculated for two vibration amplitudes, $A = 1, 2$. For both amplitudes the diffusion coefficient exhibits a resonance behavior for frequencies, which are close to the characteristic frequency, $\Omega = 1$. To gain a better insight into the mechanism of the enhanced diffusion we present in Fig. 3 trajectories of the tip for $A = 1$ and three characteristic frequencies: (i) low frequency, $\Omega = 0.30$, (ii) the resonance frequency, $\Omega_* = 0.41$, which corresponds to the maximum of the diffusion coefficient, and (iii) the frequency, $\Omega = 0.55$, that is higher than Ω_* but corresponds to a

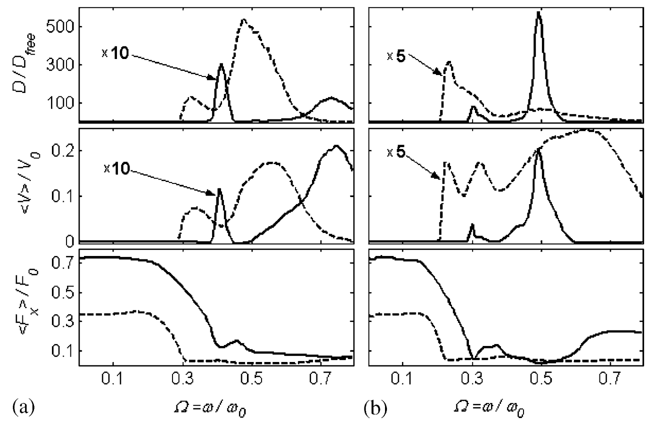

Fig. 2. Frequency dependence of the relative diffusion coefficient (top panel, $F_x \equiv 0$), the time-averaged tip velocity (middle panel, $F_x = F_{dc} = 0.01F_0$) and the friction force (bottom panel, $F_x = K_x(vt - x)$) calculated for a fixed tip–surface separation (solid curves) and including the normal motion (dashed curves); (a) $A = 1$ and (b) $A = 2$. Parameter values: $\lambda/b = 1$, $\sigma = 1$, $\eta_{x,z}/M\omega_0 = 3.2$, $k_B T/U_0 = 0.01$, $K_x b^2/(4\pi^2 U_0 \sigma) = 3.2 \times 10^{-3}$, $K_z \lambda^2/U_0 = 0.63$, $F_{dc}/F_0 = 0.01$, $v/V_0 = 0.16$, where $F_0 = 2\pi U_0/b$ and $V_0 = \omega_0 b$.

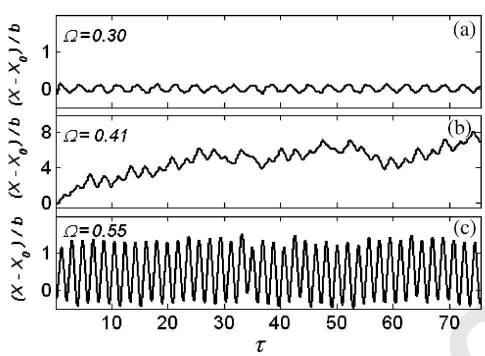

Fig. 3. Time dependences of the tip displacement calculated for three frequencies: (a) $\Omega = 0.30$, (b) $\Omega = 0.41$, (c) $\Omega = 0.55$. Parameter values: $A = 1$, $K_z \to \infty$ (a fixed tip–surface separation), other parameters as in Fig. 2.

small diffusion coefficient. For low frequencies, $\Omega \ll 1$, the tip follows the motion of the plate, performing small oscillations around the potential minima. The energy of thermal fluctuations is essentially smaller than the height of the potential barrier and as a result, the probability to escape from the potential well is exponentially small in this case. With increase in Ω, the tip has no time to respond to the substrate vibrations, and the amplitude of the tip oscillations increases. At resonance frequencies, $\Omega = \Omega_*$, which correspond to the maxima of the diffusion coefficient, the tip approaches the top of the surface potential at the end of half cycle of the plate vibrations, where the driving force, $F_{ac} = 0$. Then, even a weak thermal noise splits the ensemble of tips into two parts that relax to the neighboring minima of the surface potential, and the resonance enhancement of diffusion is observed.

In order to illustrate a nature of the resonance enhancement of the tip diffusion we show in Fig. 4 a time

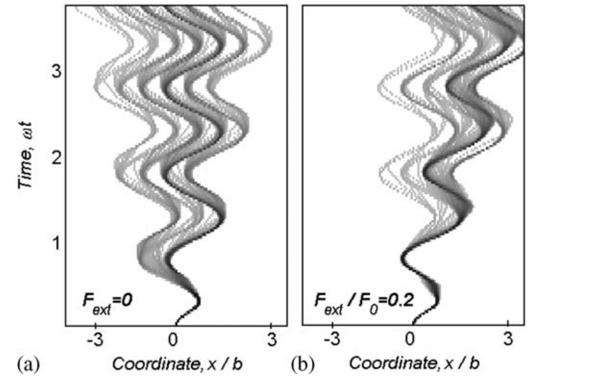

Fig. 4. Time-evolution of the density of tips interacting with a vibrating surface: (a) $F_x = 0$, (b) $F_x = 0.2F_0$. Regions with high and law density are marked by dark and light colors, respectively. Parameters values: $A = 1$; $\Omega = 0.41$, $K_z \to \infty$, other parameters as in Fig. 2.

evolution of the spatial distribution of the tips which are initially located in the potential minimum at $x = 0$. Fig. 4 shows that under the action of the oscillating driving force the ensemble of tips splits at every half cycle of the vibrations. The effect of thermal fluctuations on the tip motion leads to a broadening of the branches shown in Fig. 4. This is a manifestation of the thermally-induced fluctuations of the tip within one potential well.

Further increase of the frequency, above Ω_*, leads again to localized oscillations of the tip (see Fig. 3). In contrast to the case of low frequencies here the tip overcomes the potential barriers and oscillates between neighboring minima of the surface potential with a period equals to half of the period of the plate vibrations. In this case we observe a slippage of the tip with respect to the plate. We note that a significant slippage arises already for lower frequencies, $\Omega < \Omega_*$, at which the diffusion coefficients starts to grow as a function of Ω.

3.1.1. How to observe experimentally the enhanced diffusion?

Our calculations suggest that the vibration-induced enhancement of the diffusion can be observed in AFM experiments. In this configuration the tip experiences the influence of two potentials: the periodic surface potential and the harmonic potential, $K_x(x - x_{sup})^2/2$, due to the elastic coupling to the support of the microscope of coordinate x_{sup}, which remains fixed. Our simulations in Fig. 5 demonstrate that the experimentally measurable root mean square displacement (rmsd) of the tip, $\Delta L(\Omega)$, exhibits a resonance enhancement for the frequency Ω_* corresponding to the maximum of the diffusion coefficient. The results for $\Delta L(\Omega)$ can be fitted by the Ornstein–Uhlenbeck equation

$$\Delta L_{OU} = \sqrt{D_{free}\eta_x/K_x}$$

for the rmsd due to diffusion in the harmonic potential [25], when a free diffusion coefficient, D_{free}, is substituted by the

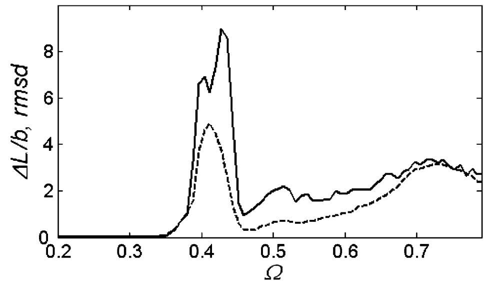

Fig. 5. Frequency dependence of the root mean squared displacement (rmsd) of the tip. Solid curve—numerical simulations, dashed curve—calculation according to the equation $\Delta L(\Omega) = \sqrt{D(\Omega)\eta_x/K_x}$. Parameter values: $A = 1$, $K_x b^2/((2\pi)^2 U_0 \sigma) = 3.2 \times 10^{-4}$, $K_z \to \infty$, other parameters as in Fig. 2.

Ω-dependent enhanced diffusion coefficient, $D(\Omega)$ (the dashed curve in Fig. 5).

Under the conditions which are typical for AFM measurements [14], $m = 8.7 \times 10^{-12}$ kg, $U_0 = 0.25$ eV and $b = 0.4$ nm, we arrive at the resonance frequency $\omega_* = \omega_0 \Omega_* = 7 \times 10^4$ Hz. This value lies within the frequency interval exploited by the shear modulation technique [18] and agrees qualitatively with the value of the frequency for which the resonance reduction of friction under the oscillatory drive has been observed [14]. The experiment suggested here can be considered as a diffusion "spectroscopy" of surfaces. Measuring "spectrum" of diffusion, $D(\Omega)$, one can determine the parameters of the surface potential.

3.1.2. Effect of normal–lateral coupling on the enhanced diffusion

In AFM experiments the tip is held near the surface by the normal load applied through the spring with the spring constant K_z. As a result the tip driven in a lateral direction performs also oscillations in the normal direction [11]. The amplitude of these oscillations depends on the surface potential and the stiffness of the normal spring. As in the one-dimensional model, we observed here a strong enhancement of diffusion under the lateral vibrations. The mechanism of the enhanced diffusion is similar to that described above.

The effect of normal oscillations of the tip on the lateral diffusion is clearly seen in Fig. 2 where we present a comparison between the Ω-dependencies of the diffusion coefficients calculated for a fixed tip–surface separation and including the normal motion. In the latter case we also observed a giant enhancement of diffusion induced by the lateral vibrations, but the shape of $D(\Omega)$ is very different from that obtained for the one-dimensional case. In order to gain insight into the effect of normal–lateral coupling on the surface diffusion we show in Fig. 6 the frequency dependence of the time-averaged distance between the tip and the surface. This figure as well as the tip trajectories (see Fig. 7) demonstrate the existence of two stable surface separations z_0 and z_h, which correspond to small tip

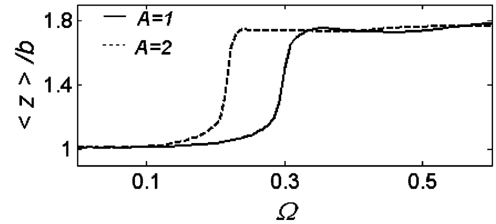

Fig. 6. Frequency dependence of the time-averaged tip–surface separation; solid curve—$A = 1$, dashed curve—$A = 2$. Parameters values as in Fig. 2.

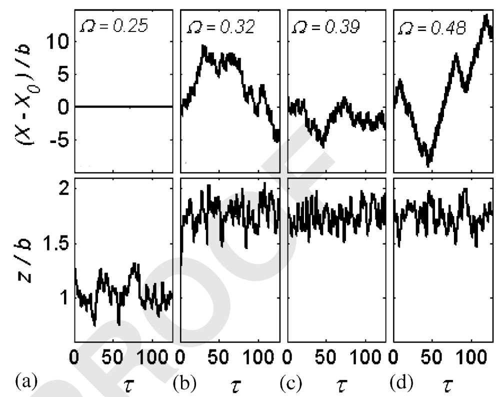

Fig. 7. Time dependencies of the lateral tip displacement (top panel) and the tip–surface separation (bottom panel) calculated for four vibration frequencies: (a) $\Omega = 0.26$, (b) $\Omega = 0.32$, (c) $\Omega = 0.39$, (d) $\Omega = 0.48$. Parameters values: $A = 1$, $K_z \lambda^2/U_0 = 0.63$, $F_x = 0$, other parameters as in Fig. 2.

oscillations in the vicinity of the potential minima (low Ω) and to the large-scale tip displacements (high Ω), respectively. The excitation of normal motion by the lateral drive becomes efficient only when the amplitude of the lateral tip oscillations is large enough to feel a nonlinearity of the tip–surface interaction. As a result, for a given driving amplitude the dilatancy is observed only for frequencies which exceed some threshold value, Ω_{th}, which depends on the potential and normal load.

Fig. 6 shows a sharp transition from the state with a small tip–surface separation to the state with a large separation which occurs with increasing frequency. It must be noted that both the dilatancy transition and enhancement of diffusion originate from the excitation of the large-scale tip oscillations by the substrate vibrations. As a result both effects arise at the same threshold frequency, Ω_{th}. However, in contrast to the dilation which takes place for all $\Omega > \Omega_{th}$, the significant enhancement of diffusion occurs only in a vicinity of the resonance frequencies for which the amplitude of tip oscillations equals to $b(1 + n/2)$, $n = 1, 2, \ldots$.

The dilatancy leads to a reduction of the amplitude of the potential corrugation and of the dissipation parameter η_x experienced by the tip. This results in a decrease of the driving frequencies and amplitudes, which correspond to the resonances of $D(\Omega)$, and to a broadening of the resonance peaks compared to the case of the constant tip–surface separation.

3.2. Vibration-induced enhancement of surface mobility

Substrate vibrations cause also a resonance enhancement of surface mobility which arises under the action of a time-independent (dc) force, $F_x \equiv F_{\mathrm{dc}}$ (see Fig. 2, middle panel). In order to illustrate a nature of the vibration-induced mobility we show in Fig. 4 a time evolution of the spatial distribution of the tips under the influence of substrate vibrations and the applied dc force. In this simulation the dc force was chosen to be significantly smaller than the maximal slope of the surface potential, F_0 ($|F_0| = \max|\partial U/\partial x| = 2\pi\sigma U_0/b$), and it does not induce a noticeable directed motion in the absence of vibrations. Similar to the case of vibration-induced diffusion, which has been discussed above, we found that the ensemble of tips splits at every half cycle of the vibrations. However, in contrast to the previous case the presence of the force results into an asymmetric splitting that leads to a pronounced drift of the ensemble in the direction of the applied force.

There is a clear correlation between the enhancement of diffusion and time-averaged tip velocity, $\langle V \rangle$ (see Fig. 2). In the case of regular diffusion caused by the equilibrium thermal fluctuations, the fluctuation dissipation theorem suggests that there is a linear relation between the diffusion coefficient and the average velocity calculated in the limit of zero dc driving, $D = k_{\mathrm{B}}T(\mathrm{d}\langle V\rangle/\mathrm{d}F_{\mathrm{dc}})|_{F_{\mathrm{dc}}=0}$. The reason why we do not observe the proportionality relation here is that the enhanced diffusion is induced by the *nonequilibrium* vibrations, and the fluctuation dissipation theorem breaks down in this case. It should be also noted that the calculations have been done for a small but finite driving force, that can also violate the proportionality between D and $\langle V \rangle$.

3.3. Vibration-induced reduction of friction

The calculations performed for a dc driving force can simulate the AFM frictional response in the limit of a very weak lateral spring, $K_x \to 0$ where the applied force, $F_x = K_x(vt - x)$, remains almost constant. However, for low driving velocities where a stick–slip motion is usually observed [14,15], a time variation of F_x should be taken into account. Below we focus on the effect of lateral vibrations on this regime of motion.

Figs. 2 (bottom panel) and 8 show the Ω-dependence of the time-averaged friction force, $\langle F_x \rangle$, and the instantaneous friction force, $F_x = K_x(vt - x)$, tip displacement and tip–surface separation, respectively. One can see that, for low frequencies the lateral vibrations do not affect the frictional response. Both the spring force and displacement traces show the patterns which are typical for the stick–slip behavior, and the average force is independent of Ω. The maximal value of the force (static friction) is determined by the maximal slope of the surface potential, $F_0 = 2\pi U_0/b$. The effect of thermal fluctuations leads to a reduction of the static friction compared to F_0.

For a finite stiffness of the normal spring the tip–surface separation, which is initially z_0, at equilibrium, starts growing before a slippage occurs and stabilizes at a larger distance, z_{h}, as long as the motion continues (see Fig. 8). Since the static friction is determined by the amplitude of the potential corrugation, it is obvious that the dilatancy leads to a decrease of the static friction compared to the case of a constant tip–surface distance (see Fig. 2, bottom panel).

In the vicinity of the threshold frequency Ω_{th} for which the enhanced diffusion is beginning to emerge, we find a drastic decrease of the kinetic friction. Figs. 2 and 8 demonstrate that the lateral vibrations not only reduce the friction force but they also transform the stick–slip motion to a "smooth" sliding. However, the application of lateral vibrations does not allow to eliminate completely the force fluctuations. Even under the optimal conditions the variance of the friction force remains of the order of K_xA. The transition in the lateral response is accompanied by a dilatancy transition (see Fig. 8).

The main feature in Fig. 2 (bottom panel) is a reduction of friction for all frequencies above the threshold one, Ω_{th}. In contrast to the enhancement of diffusion and mobility, the reduction of friction does not exhibit pronounced resonance features. This is a consequence of the fluctuations of the applied force. Contrary to the calculations of the mobility, which have been done for a small constant force, in the configuration corresponding to the friction experiments the fluctuations of the applied force are of the order of K_xA, and they can be essentially larger than the average value of the force. For $\Omega > \Omega_{\mathrm{th}}$ where the substrate vibrations induce large-scale oscillations of the tip, these fluctuations are sufficient to cause a slow motion of the tip.

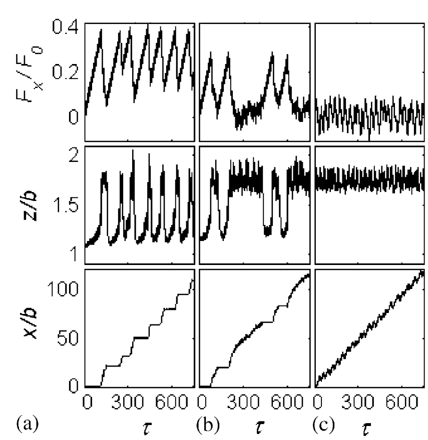

Fig. 8. Time dependencies of the relative friction force, F_x/F_0, the tip–surface separation, z/b, and the tip displacement, x/b calculated for $A = 1$ and three frequencies: $\Omega = 0.26$ (a), 0.29 (b), and 0.32 (c). Parameters value as in Fig. 2.

Our calculations show that the lateral vibrations can lead to the essential reduction of friction only in a range of low driving velocities where the rate of increase of the driving force is much smaller than the frequency of the vibrations, $K_x V/\omega \ll F_0$. AFM measurement [14] also demonstrated that for high driving velocities the lateral vibration only slightly influence friction.

Including a normal motion of the tip does not change qualitatively the effect of vibrations on friction. As in the one-dimensional case, the main feature of the frequency dependence of frictional force is a sharp decrease of $\langle F \rangle$ and the transition from the stick–slip motion to sliding at the threshold frequency, Ω_{th}. The threshold frequency decreases with a decrease of the stiffness of the normal spring, K_z. In the majority of cases a decrease of K_z leads also to a reduction of the time-averaged frictional force, $\langle F \rangle$. This can be easily understood, because the decrease of the stiffness, K_z, results in the reduction of the actual amplitude of the surface potential experienced by the tip.

4. Conclusion

In summary, we have demonstrated that lateral vibrations of the substrate can dramatically increase surface diffusivity and mobility and reduce friction at the nanoscale. In contrast to the enhancement of diffusion and mobility that has a resonance nature, the reduction of friction does not exhibit pronounce resonance features. We have studied the effect of normal motion of the tip which is induced by the lateral vibrations on the surface diffusion, mobility and friction. We have found a sharp transition from the state with a small tip–surface separation to the state with a large separation as the vibration frequency increases. This strongly influences the dependences of vibration-induced diffusion, mobility and friction on the frequency and amplitude of the substrate vibrations. The predicted effects should be amenable to AFM tests using, for instance, shear modulation mode [14,19] or applying ultrasound to the sample [20,21].

Acknowledgment

The authors are grateful to Joseph Klafter for fruitful discussions. This research was supported by the Israel Science Foundation and by Deutsche Forschungsgemeinschaft (HA 1517/26-1). A. E. F thanks the ESF "Nanotribology" Program for financial support.

References

[1] Metzler R, Klafter J. The restaurant at the end of the random walk: recent developments in the description of anomalous transport by fractional dynamics. J Phys A: Math Gen 2004;37(31):R161–208.

[2] Fourkas JT, Levitz PE, Urbakh M, Wahl KJ, editors. Dynamics in small confining systems. Pittsburgh: Material Research Society; 2003.

[3] Persson BNJ. Sliding friction, physical properties and applications. Berlin: Springer; 2000.

[4] Urbakh M, Klafter J, Gourdon D, Israelachvili J. The nonlinear nature of friction. Nature 2004;430(6999):525–8.

[5] Astumian RD, Hanggi P. Brownian motors. Phys Today 2002;55(11):33–9.

[6] Gang H, Daffertshofer A, Haken H. Diffusion of periodically forced Brownian particles moving in space-periodic potentials. Phys Rev Lett 1996;76(26):4874–7.

[7] Schreier M, Reimann P, Hanggi P, Pollak E. Giant enhancement of diffusion and particle selection in rocked periodic potentials. Europhys Lett 1998;44(4):416–22.

[8] Rozman MG, Urbakh M, Klafter J. Controlling chaotic frictional forces. Phys Rev 1998;E 57(6):7340–3.

[9] Gao JP, Luedtke WD, Landman U. Friction control in thin-film lubrication. J Phys Chem 1998;B 102(26):5033–7.

[10] Heuberger M, Drummond C, Israelachvili J. Coupling of normal and transverse motions during frictional sliding. J Phys Chem 1998;B 102(26):5038–41.

[11] Zaloj V, Urbakh M, Klafter J. Modifying friction by manipulating normal response to lateral motion. Phys Rev Lett 1999;82(24):4823–6.

[12] Braiman Y, Barhen J, Protopopescu V. Control of friction at the nanoscale. Phys Rev Lett 2003;90(9) Art. No. 94301.

[13] Cochard A, Bureau L, Baumberger T. Stabilization of frictional sliding by normal load modulation. J Appl Mech Trans ASME 2003;70(2):220–6.

[14] Riedo E, Gnecco E, Bennewitz R, Meyer E, Brune H. Interaction potential and hopping dynamics governing sliding friction. Phys Rev Lett 2003;91(8) Art. No. 084502.

[15] Muser MH, Urbakh M, Robbins MO. Statistical mechanics of static and low-velocity kinetic friction. Adv Chem Phys 2003;126:188–272.

[16] Dudko O, Filippov AE, Klafter J, Urbakh M. Chemical control of friction: mixed lubricant monolayers. Trib Lett 2002;12(4):217–27.

[17] Mosey NJ, Muser MH, Woo TK. Molecular mechanisms for the functionality of lubricant additives. Science 2005;305(5715):1612–5.

[18] Tshiprut Z, Filippov AE, Urbakh M. Tuning diffusion and friction in microscopic contacts by mechanical excitations. Phys Rev Lett 2005;95(1):016101.

[19] Ge S, Pu Y, Zhang W, Rafailovich M, Sokolov J, Buenviaje C, Buckmaster R, Overney RM. Shear modulation force microscopy study of near surface glass transition temperatures. Phys Rev Lett 2000;85(11):2340–3.

[20] Dinelli F, Biswas SK, Briggs GAD, Kolosov OV. Ultrasound induced lubricity in microscopic contact. Appl Phys Lett 1997;71(9):1177–9.

[21] Hesjedal T, Behme G. The origin of ultrasound-induced friction reduction in microscopic mechanical contacts. IEEE Trans Ultrason Ferroel Freq Contr 2002;49(3):356–64.

[22] Borovsky B, Krim J, Syed Asif SA, Wahl KJ. Measuring nanomechanical properties of a dynamic contact using an indenter probe and quartz crystal microbalance. J Appl Phys 2001;90(12):6391–6.

[23] Berg S, Johannsmann D. High speed microtribology with quartz crystal resonators. Phys Rev Lett 2003;91(14) Art. No. 145505.

[24] Lubben JF, Johannsmann D. Nanoscale high-frequency contact mechanics using an AFM tip and a quartz crystal resonator. Langmuir 2004;20(9):3698–703.

[25] Risken H. The Fokker–Planck equation. Berlin: Springer; 1996.